

Viscous corrections to anisotropic flow and transverse momentum spectra from transport theory

Salvatore Plumari,^{1,2} Giovanni Luca Guardo,^{1,2} Vincenzo Greco,^{1,2} and Jean-Yves Ollitrault³

¹*Department of Physics and Astronomy, University of Catania, Via S. Sofia 64, I-95125 Catania*

²*Laboratorio Nazionale del Sud, INFN-LNS, Via S. Sofia 63, I-95125 Catania*

³*Institut de physique théorique, Université Paris Saclay, CNRS, CEA, F-91191 Gif-sur-Yvette, France*

(Dated: May 25, 2022)

Viscous hydrodynamics is commonly used to model the evolution of the matter created in an ultra-relativistic heavy-ion collision. It provides a good description of transverse momentum spectra and anisotropic flow. These observables, however, cannot be consistently derived using viscous hydrodynamics alone, because they depend on the microscopic interactions at freeze-out. We derive the ideal hydrodynamic limit and the first-order viscous correction to anisotropic flow (v_2 , v_3 and v_4) and momentum spectrum using a transport calculation. The linear response coefficient to the initial anisotropy, $v_n(p_T)/\varepsilon_n$, depends little on n in the ideal hydrodynamic limit. The viscous correction to the spectrum depends not only on the differential cross section, but also on the initial momentum distribution. This dependence is not captured by standard second-order viscous hydrodynamics. The viscous correction to anisotropic flow increases with p_T , but this increase is slower than usually assumed in viscous hydrodynamic calculations. In particular, it is too slow to explain the observed maximum of v_n at $p_T \sim 3$ GeV/c.

I. INTRODUCTION

Relativistic viscous hydrodynamics [1, 2] is the state of the art for describing the evolution of the strongly-coupled system formed in an ultrarelativistic heavy-ion collision at RHIC or LHC. It has long been realized [3] that ideal hydrodynamics naturally explains the large magnitude of elliptic flow [4, 5]. However, the system formed in such a collision is so small that deviations from local thermal equilibrium are sizable, resulting in the inclusion of viscosity [6] in hydrodynamic calculations. Viscosity typically reduces the magnitude of elliptic flow by 20% [7]. Viscous effects on higher harmonics of anisotropic flow [8, 9], such as triangular flow [10], are even larger [11].

Even though there is a consensus that viscosity matters, the calculation of viscous corrections to observables is not yet under control. The reason is that viscosity affects not only the space-time history of the fluid [12], but also the momentum distribution of particles at “freeze-out”, which has an off-equilibrium part proportional to viscosity [13, 14]. Viscous hydrodynamics itself does not fully specify this off-equilibrium part. The only requirement is that the system of particles should generate the same energy-momentum tensor as the fluid just before freeze out [15]. This requirement, however, does not constrain the dependence of the relative deviation to equilibrium on the momentum p in the rest frame of the fluid, which is essentially a free function $\chi(p)$. This function is not universal, and involves the differential cross sections between constituents [16]. It is typically put by hand in hydrodynamic calculations.

The common lore is that effects of viscosity are more important for particles with larger transverse momenta [2]. This is due to the fact that most hydrodynamic calculations use the “quadratic” ansatz [13] $\chi(p) \propto$

p^2 . While this choice generally results in a improved description of experimental data [2] (see however [15]), it is not supported by any theoretical argument [16]. We evaluate viscous corrections to observables (specifically, transverse momentum spectra and anisotropic flow) by solving numerically a relativistic Boltzmann equation. We simulate relativistic particles undergoing $2 \rightarrow 2$ elastic collisions with a total cross section σ_{tot} . In the limit $\sigma_{\text{tot}} \rightarrow +\infty$, a generic observable $f(\sigma)$ can be expanded in powers of $1/\sigma_{\text{tot}}$:

$$f(\sigma_{\text{tot}}) \underset{\sigma_{\text{tot}} \rightarrow \infty}{\approx} f^{(0)} + \frac{1}{\sigma_{\text{tot}}} \delta f + \mathcal{O}\left(\frac{1}{\sigma_{\text{tot}}^2}\right). \quad (1)$$

The leading term $f^{(0)}$ is the limit of infinite cross section, which corresponds to ideal hydrodynamics in the limit of a vanishing freeze-out temperature [17, 18]. The next-to-leading term δf is a viscous correction: since the shear viscosity η scales like $1/\sigma_{\text{tot}}$ [19], this correction is proportional to η .¹

We evaluate $f^{(0)}$ and δf by solving numerically the relativistic Boltzmann equation for several large values of the cross section σ_{tot} . Our primary goal is to illustrate by an explicit calculation how the viscous correction to anisotropic flow depends on transverse momentum p_T , and to what extent this dependence is sensitive to the structure of the differential cross section. We do not mean here to carry out a full realistic simulation of a heavy-ion collision. In particular, for sake of simplicity, our transport calculation uses massless particles which supply the possibility of having only shear viscosity with

¹ Note that in hydrodynamic calculations, δf often denotes the viscous correction at freeze-out. Here, δf is the full viscous correction, which also contains a contribution from the hydrodynamic evolution.

no bulk viscosity [20–22]. The resulting equation of state is harder [23] than that of QCD near the deconfinement crossover [24]. This results in larger v_n and harder p_T spectra.

We also study the dependence of observables on initial conditions. In second-order viscous hydrodynamics, the evolution is completely specified by the initial value of the energy-momentum tensor $T^{\mu\nu}$ [2, 12]. At the microscopic level, however, the initial momentum distribution contains more information than just $T^{\mu\nu}$. Usual viscous hydrodynamics assumes that this additional information is washed out by the system evolution. Our simulation provides a means of testing this assumption, by constructing two different initial conditions with the exact same $T^{\mu\nu}$, and comparing the observables at the end of the evolution.

II. INITIAL CONDITIONS AND EVOLUTION

Initial conditions follow Bjorken’s boost-invariant prescription [25], but with a finite extent in space-time rapidity $-2.5 < \eta < 2.5$. The evolution is started at time $\tau_0 = 0.6$ fm/c [26] after the collision. The initial conditions of the Boltzmann equation are specified by the one-body density $f(x, p)$ in coordinate (x) and momentum (p) space at time τ_0 .

The initial density profile in transverse coordinate space (x, y) is taken from an optical Glauber [27] calculation for a central Au-Au collision at $\sqrt{s} = 200$ GeV, corresponding to the top RHIC energy. This initial density is azimuthally symmetric, so that anisotropic flow vanishes by construction. We introduce anisotropy artificially by deforming the initial distribution, thus mimicking an initial state fluctuation [10]. In hydrodynamics, one typically deforms the initial energy density profile [11, 28]. In a transport calculation, where the initial conditions are specified by the initial positions of particles, it is simpler to just shift these positions by a small amount. Introducing the complex notation $z = x + iy$, in order to generate flow in harmonic n , we shift z according to

$$z \rightarrow z + \delta z \equiv z - \alpha \bar{z}^{n-1}, \quad (2)$$

where $\bar{z} \equiv x - iy$, and α is a real positive quantity chosen in such a way that the correction is small. This transformation is invariant under the change $z \rightarrow e^{2i\pi/n} z$, i.e., it has $2\pi/n$ symmetry. Therefore, to leading order in α , the only nonvanishing anisotropic flow coefficient is v_n .² The initial eccentricity in harmonic n is defined for $n \geq 2$

by [29, 30]

$$\varepsilon_n \equiv -\frac{\sum_j (z_j + \delta z_j)^n}{\sum_j |z_j + \delta z_j|^n}, \quad (3)$$

where the sum runs over all particles with initial position z_j . Inserting Eq. (2) into Eq. (3), and using the fact that the distribution of z_j is azimuthally symmetric, one obtains, to leading order in α and for a large number of particles

$$\begin{aligned} \varepsilon_n &\simeq -\frac{\sum_j n z_j^{n-1} \delta z_j}{\sum_j |z_j|^n} = n\alpha \frac{\sum_j |z_j|^{2(n-1)}}{\sum_j |z_j|^n} \\ &\simeq n\alpha \frac{\langle r^{2(n-1)} \rangle}{\langle r^n \rangle}, \end{aligned} \quad (4)$$

where, in the right-hand side, angular brackets denote an average taken with the optical Glauber profile, and $r = |z| = \sqrt{x^2 + y^2}$. We carry out simulations for $n = 2, 3, 4$. For each n , we fix α in such a way that $\varepsilon_n = 0.2$. We have checked that this value is sufficiently small that the response is linear [11]. In hydrodynamics with fluctuating initial conditions, v_2 and v_3 are determined to a good approximation by linear response to the eccentricity in the corresponding harmonic [31, 32]. On the other hand, v_4 is the superposition of a linear term [33], and a nonlinear term induced by v_2 [34]. The present study only addresses the linear term.

In momentum space, we consider two different types of initial conditions. The first case is a thermal Boltzmann distribution

$$dN/d^3p \propto \exp(-p/T). \quad (5)$$

In addition, one requires that the temperature T and the local density n be such that n/T^3 is a constant throughout the transverse plane, as in a thermal gas of massless particles with zero chemical potential. Thus this initial condition is that of a hydrodynamic calculation with zero chemical potential [23]. The initial temperature at the center of the fireball is $T_0 = 340$ MeV. The second case is a constant distribution:

$$dN/d^3p \propto \theta(p_0 - p). \quad (6)$$

The maximum momentum p_0 and the proportionality constant are chosen such that the particle density n and the energy density ε are the same as with the previous initial condition. Similar initial conditions have been previously used in transport calculations in order to mimic the effect of saturation in high-energy QCD [35, 36]. Both types of initial conditions have exactly the same energy-momentum tensor.

The evolution of the system is determined by the relativistic classical Boltzmann equation. We use a relativistic transport code developed to study heavy-ion collisions at RHIC and LHC energies [19, 37–41], which uses the test-particle method. The collision integral is solved by using Monte Carlo methods based on the stochastic interpretation of transition amplitudes [19, 37, 42]. The

² Note that the deformation used in Refs. [11, 28] is singular at the origin $z = 0$ for $n \neq 2$. By contrast, the deformation defined by Eq. (2) is regular at the origin, but has a singularity at large $|z|$ (see also [29]). On the x axis, the singularity is located at the point where $\partial\delta x/\partial x = -1$. If α is small, this singularity occurs at a point where the density is low.

total cross section is fixed throughout the evolution. The differential cross section is

$$\frac{d\sigma}{dt} \propto \frac{1}{(t - m_D^2)^2}, \quad (7)$$

where t is the usual Mandelstam variable. This differential cross section is typically used in parton cascade approaches [37, 38, 42–44] and by symmetry the u -channel is included. The limit $m_D \rightarrow \infty$ corresponds to an isotropic cross section. The opposite limit, where m_D is smaller than the typical particle energy, corresponds to a forward-peaked cross section.

In a transport approach, one can follow the evolution of the system until the last collision, but this is numerically expensive. Instead, we choose to follow the system until a fixed final time, and check stability of our results with respect to this final time. The calculations presented in this paper are carried out with a final time $t_f = 8 \text{ fm}/c$, but we have checked that the momentum spectra are unchanged if we extend the final time to $t_f = 12 \text{ fm}/c$. Since the initial density profile possesses $\phi \rightarrow -\phi$ symmetry (where ϕ is the azimuthal angle), we define anisotropic flow as $v_n = \langle \cos n\phi \rangle$, where angular brackets denote an average over particles at the end of the evolution.

Throughout this paper, we carry out four sets of calculations: Three sets with the thermal initial distribution (5) and the values $m_D = 0.3 \text{ GeV}$, $m_D = 0.7 \text{ GeV}$ and an isotropic cross section, and a fourth set with the constant initial distribution (6) and an isotropic cross section. Thus we study how results depend on the initial distribution and on the differential cross section.

For each set of parameters, we perform different calculations for the following set of total cross sections: $\sigma_{\text{tot}} = 20, 25, 30$ and 35 mb . Results for anisotropic flow v_n [1] are shown in Fig. 1. The dependence of these observables on $1/\sigma_{\text{tot}}$ is essentially linear, corresponding to the regime where viscous hydrodynamics applies. In order to improve the accuracy, we fit these results with a polynomial of order 2 in $1/\sigma_{\text{tot}}$ and extract the ideal hydrodynamic limit and the first viscous correction using Eq. (1): specifically, the ideal hydrodynamic limit $f^{(0)}$ is the extrapolation to $1/\sigma_{\text{tot}} \rightarrow 0$ and the viscous correction δf is the slope at the origin.

III. IDEAL HYDRODYNAMICS

We first study the ideal hydrodynamic limit, defined by the extrapolation $\sigma_{\text{tot}} \rightarrow +\infty$ in the Boltzmann equation. Ideal hydrodynamics corresponds to local thermal equilibrium [23]. One expects thermalization to wash out details of initial conditions, so that observables should not depend on the initial momentum spectrum provided the energy density is fixed. Similarly, the momentum distribution in thermal equilibrium is universal, therefore one expects observables to be independent of the differential cross section in this limit.

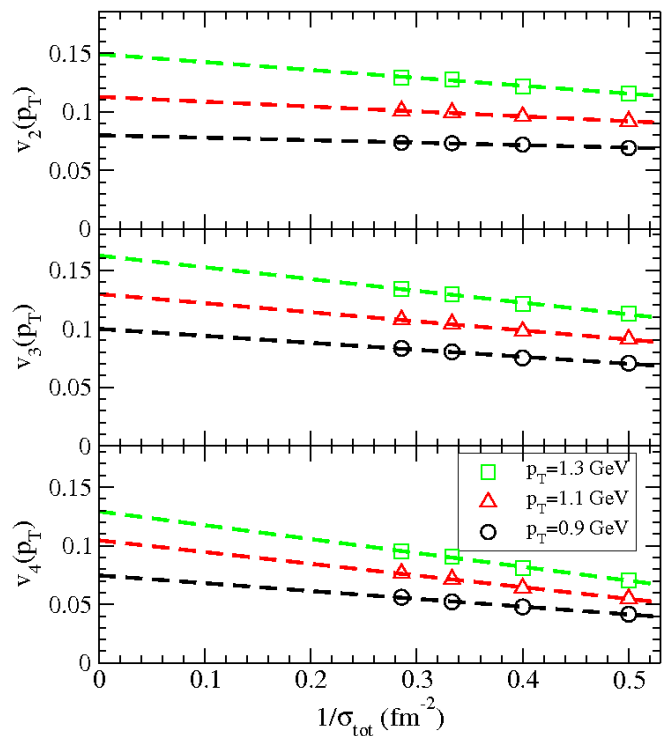


FIG. 1. Left panel: $v_n(p_T)$ as a function of $1/\sigma_{\text{tot}}$ (thermal initial distribution, isotropic scattering cross section) in the rapidity interval $|y| < 0.5$. The y -intercept is the ideal hydrodynamic limit $v_n^{(0)}$, while the slope corresponds to the viscous correction δv_n , as defined by Eq. (1).

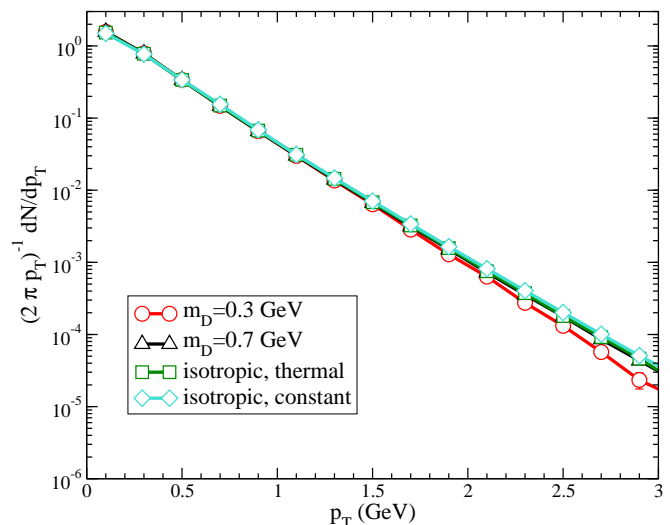


FIG. 2. Ideal hydrodynamic limit for the p_T spectrum in the rapidity interval $|y| < 0.5$. The spectra have been divided by dN/dy so that they are normalized to unity.

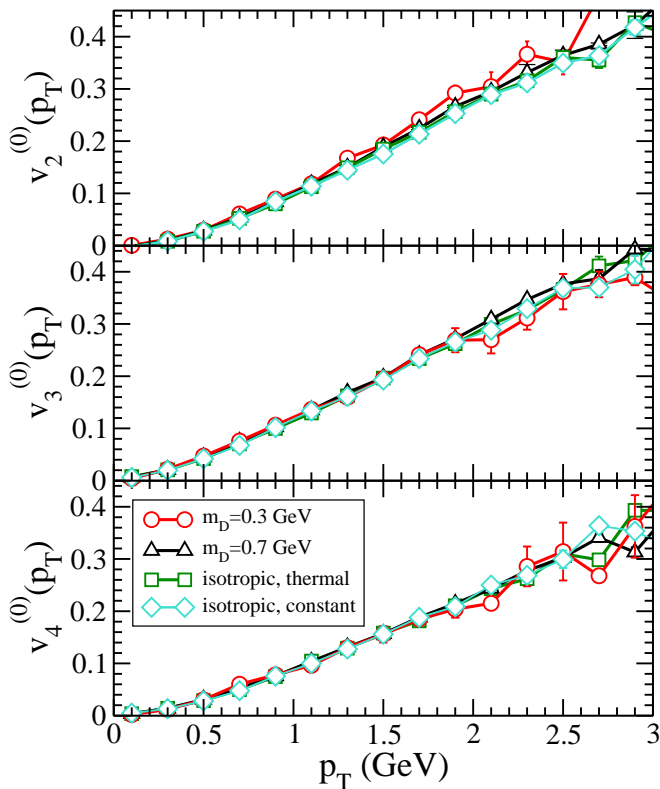


FIG. 3. Ideal hydrodynamic limit of anisotropic flow v_n . Top to bottom: $n = 2, 3, 4$. For all harmonics, we have chosen $\varepsilon_n = 0.2$, so that the linear response coefficients $\kappa_n \equiv v_n/\varepsilon_n$ are larger by a factor 5.

Figure 2 displays the ideal hydrodynamic limit for the transverse momentum distribution in the rapidity interval $|y| < 0.5$. As expected, it is independent of initial conditions and of the differential cross section. The distribution is essentially exponential in p_T , with a slight upward curvature which is a typical consequence of collective motion [3, 45]. The ideal hydrodynamic limit of anisotropic flow coefficients is displayed in Fig. 3. $v_n(p_T)$ is linear at high p_T , as observed in previous numerical calculations [11]. This behavior is general in ideal hydrodynamics [33] in the linear regime $\varepsilon_n \ll 1$. Interestingly, the magnitude of the linear response $\kappa_n(p_T) \equiv v_n(p_T)/\varepsilon_n$ [46] is approximately the same for $n = 2, 3, 4$. It would be interesting to reproduce these results using ideal hydrodynamics with the same ideal gas equation of state (constant sound velocity $c_s = 1/\sqrt{3}$) and a small freeze-out temperature.

IV. VISCOUS CORRECTION

We now present results for the first-order viscous correction to observables, corresponding to the term δf in Eq. (1). We scale the viscous correction δf by the ideal hydrodynamic limit $f^{(0)}$. Eq. (1) shows that $\delta f/f^{(0)}$ has

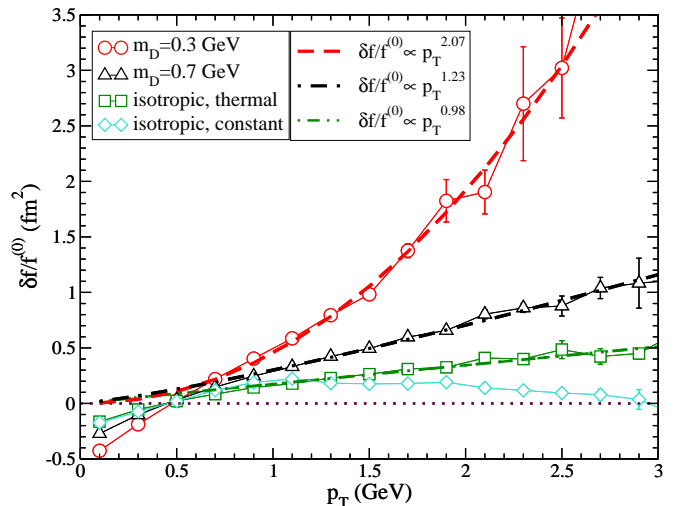


FIG. 4. First-order relative viscous correction to the normalized transverse momentum distribution in the rapidity interval $|y| < 0.5$. Dashed lines are power-law fits.

the dimension of the cross section σ_{tot} . The relative viscous correction is $\delta f/f^{(0)}$ divided by the total cross section σ_{tot} . As a rule of thumb, viscous hydrodynamic applies if $\delta f/f^{(0)}$ is significantly smaller than σ_{tot} in absolute value.

Figure 4 displays $\delta f/f^{(0)}$ for the transverse momentum spectrum. Viscous effects result in a particle excess at large p_T , corresponding to an increase of the average p_T , that is, a higher effective temperature. The reason is that viscosity decreases the longitudinal pressure, thereby reducing longitudinal cooling[47, 48].

Unlike the ideal hydrodynamic limit, the first-order viscous correction depends on the differential cross section. It is larger for smaller values of m_D . This is due to the fact that the scattering is forward peaked and less efficient in thermalizing the system. For an isotropic cross section, the relative viscous correction is almost linear in p_T : $\delta f/f^{(0)} \propto p_T^{0.98}$. This result is consistent with the results obtained in [49] in the Chapman-Enskog approximation.

Surprisingly, the viscous correction also depends on the initial momentum distribution. Two initial conditions with exactly the same energy-momentum tensor $T^{\mu\nu}$ lead to different first-order viscous corrections to observables, at variance with usual viscous hydrodynamics [12]. The reason is that the constant momentum distribution (6) is strongly out of equilibrium, therefore hydrodynamics does not apply at early times. Figure 4 shows that with this constant distribution, δf is smaller at high p_T than with a thermal initial distribution. This depletion at high p_T can be understood as a memory of the initial conditions, where all particles initially have momenta below a threshold p_0 .

Finally, we study the viscous correction to anisotropic flow $v_n(p_T)$. Figure 5 displays $-\delta v_n/v_n^{(0)}$ as a function

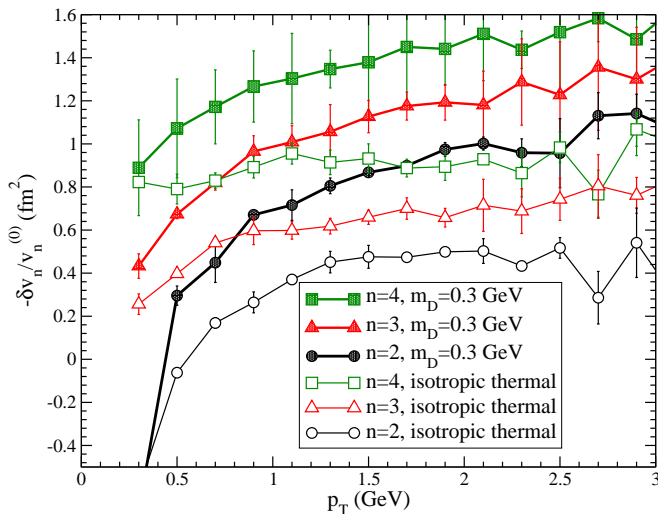


FIG. 5. $-\delta v_n(p_T)/v_n^{(0)}$ as a function of transverse momentum p_T in the rapidity interval $|y| < 0.5$. Open symbols refer to the case of isotropic cross section and full symbols to a forward-peaked cross section. The circles, triangles and squares refer to $n = 2, 3$ and 4 respectively.

of transverse momentum p_T . Viscous effects decrease anisotropic flow [13], therefore the correction is shown with a minus sign. The viscous correction to v_n increases as a function of harmonic order n , as already observed in viscous hydrodynamic calculations [11]. At large transverse momentum, it scales approximately like the order n [50], $-\delta v_n(p_T)/v_n^{(0)} \propto n$. This dependence is weaker than the n^2 dependence reported in previous studies [33, 51–53].

As expected, the viscous correction depends on the differential cross section. As for the spectrum, it is larger with a forward-peaked cross section ($m_D = 0.3$ GeV) than with an isotropic cross section. Results with the thermal distribution (5) and with the constant distribution (6) (not shown) are consistent within error bars, thereby suggesting that the viscous correction to v_n is roughly independent of the initial momentum distribution.

With an isotropic cross section, the relative viscous correction saturates at high p_T , while the usual quadratic freeze-out ansatz [13] predicts a linear increase. A mild increase with p_T is observed with a forward-peaked cross section, but it is still much slower than linear. Note that our viscous correction must be compared with the full viscous correction in hydrodynamics, which results in part from the hydrodynamic evolution, and in part from the freeze-out. With a quadratic freeze-out ansatz, however, the behavior of v_n at large p_T in hydrodynamics is dominated by the correction at freeze-out. Thus the quadratic freeze-out ansatz currently used in most

viscous hydrodynamic calculations is not supported by microscopic transport calculations.

V. CONCLUSIONS

We have calculated the ideal hydrodynamic limit and the first-order viscous correction for the transverse momentum (p_T) distribution transverse-momentum spectra and anisotropic flow $v_n(p_T)$ by solving numerically a Boltzmann equation and studying the limit of large scattering cross section $\sigma_{\text{tot}} \rightarrow \infty$. The ideal hydrodynamic limit is found to be independent of microscopic details, as expected from the universality of thermodynamic behavior. The linear response coefficients $v_n(p_T)/\varepsilon_n$ depends little on harmonic n in the ideal hydrodynamic limit.

The first order viscous corrections to observables, on the other hand, are not universal. As expected [16], they depend on the differential cross section. For all the differential cross sections investigated in this paper, we find that the relative viscous correction to anisotropic flow, v_n , does not increase significantly with p_T at large p_T . Our results suggest that first-order viscous corrections do *not* explain the decrease of v_n at high p_T , at variance with common lore [2], and that a different mechanism, such as jet quenching [54], is needed at high p_T .

The viscous correction to v_n increases linearly with n . The stronger (n^2) dependence typically found in hydrodynamics [33] leads to negative values of v_4 and v_5 at large p_T [14], even for small viscosities. A weaker dependence on harmonic n is therefore likely to improve agreement with experimental data.

Finally, our results clearly show that usual, second-order relativistic hydrodynamics does not fully capture the first-order viscous correction to observables. Two initial conditions with exactly the same energy-momentum tensor, which would therefore yield the exact same hydrodynamical flow, are found to yield different momentum spectra at the end of the evolution. Specifically, the first-order viscous correction is found to retain the memory of the initial condition. Within a strong coupling calculation, a proper treatment of the underlying microscopic degrees of freedom leads to an evolution equation which is second-order rather than first-order [56], so that the solution is not solely determined by the initial value of $T^{\mu\nu}$. Our calculation provides an explicit illustration, within a weak-coupling calculation, that the initial value of $T^{\mu\nu}$ does not solely determine the evolution.

ACKNOWLEDGMENTS

V.G. and G.L.G. acknowledge support by the European Research Council under the grant ERC QGPDyn-259684. JYO thanks Esteban Calzetta, François Gelis, Romuald Janik, Matthew Luzum and Li Yan for discussions.

-
- [1] U. Heinz and R. Snellings, *Ann. Rev. Nucl. Part. Sci.* **63**, 123 (2013) [arXiv:1301.2826 [nucl-th]].
- [2] C. Gale, S. Jeon and B. Schenke, *Int. J. Mod. Phys. A* **28**, 1340011 (2013) [arXiv:1301.5893 [nucl-th]].
- [3] P. F. Kolb and U. W. Heinz, In *Hwa, R.C. (ed.) et al.: Quark gluon plasma* 634-714 [nucl-th/0305084].
- [4] S. S. Adler *et al.* [PHENIX Collaboration], *Phys. Rev. Lett.* **91**, 182301 (2003) [nucl-ex/0305013].
- [5] K. Aamodt *et al.* [ALICE Collaboration], *Phys. Rev. Lett.* **105**, 252302 (2010) [arXiv:1011.3914 [nucl-ex]].
- [6] P. Romatschke and U. Romatschke, *Phys. Rev. Lett.* **99**, 172301 (2007) [arXiv:0706.1522 [nucl-th]].
- [7] M. Luzum and P. Romatschke, *Phys. Rev. C* **78**, 034915 (2008) [Erratum-ibid. *C* **79**, 039903 (2009)] [arXiv:0804.4015 [nucl-th]].
- [8] K. Aamodt *et al.* [ALICE Collaboration], *Phys. Rev. Lett.* **107**, 032301 (2011) [arXiv:1105.3865 [nucl-ex]].
- [9] A. Adare *et al.* [PHENIX Collaboration], *Phys. Rev. Lett.* **107**, 252301 (2011) [arXiv:1105.3928 [nucl-ex]].
- [10] B. Alver and G. Roland, *Phys. Rev. C* **81**, 054905 (2010) [Erratum-ibid. *C* **82**, 039903 (2010)] [arXiv:1003.0194 [nucl-th]].
- [11] B. H. Alver, C. Gombeaud, M. Luzum and J. Y. Ollitrault, *Phys. Rev. C* **82**, 034913 (2010) [arXiv:1007.5469 [nucl-th]].
- [12] R. Baier, P. Romatschke, D. T. Son, A. O. Starinets and M. A. Stephanov, *JHEP* **0804**, 100 (2008) [arXiv:0712.2451 [hep-th]].
- [13] D. Teaney, *Phys. Rev. C* **68**, 034913 (2003) [nucl-th/0301099].
- [14] D. Teaney and L. Yan, *Phys. Rev. C* **89**, no. 1, 014901 (2014) [arXiv:1304.3753 [nucl-th]].
- [15] M. Luzum and J. Y. Ollitrault, *Phys. Rev. C* **82**, 014906 (2010) [arXiv:1004.2023 [nucl-th]].
- [16] K. Dusling, G. D. Moore and D. Teaney, *Phys. Rev. C* **81**, 034907 (2010) [arXiv:0909.0754 [nucl-th]].
- [17] N. Borghini and J. Y. Ollitrault, *Phys. Lett. B* **642**, 227 (2006) [nucl-th/0506045].
- [18] C. Gombeaud and J. Y. Ollitrault, *Phys. Rev. C* **77**, 054904 (2008) [nucl-th/0702075].
- [19] S. Plumari, A. Puglisi, F. Scardina and V. Greco, *Phys. Rev. C* **86**, 054902 (2012) [arXiv:1208.0481 [nucl-th]].
- [20] A. Monnai and T. Hirano, *Phys. Rev. C* **80**, 054906 (2009) [arXiv:0903.4436 [nucl-th]].
- [21] P. Bozek, *Phys. Rev. C* **81**, 034909 (2010) [arXiv:0911.2397 [nucl-th]].
- [22] J. Noronha-Hostler, G. S. Denicol, J. Noronha, R. P. G. Andrade and F. Grassi, *Phys. Rev. C* **88**, 044916 (2013) [arXiv:1305.1981 [nucl-th]].
- [23] J. Y. Ollitrault, *Eur. J. Phys.* **29**, 275 (2008) [arXiv:0708.2433 [nucl-th]].
- [24] S. Borsanyi, Z. Fodor, C. Hoelbling, S. D. Katz, S. Krieg and K. K. Szabo, *Phys. Lett. B* **730**, 99 (2014) [arXiv:1309.5258 [hep-lat]].
- [25] J. D. Bjorken, *Phys. Rev. D* **27**, 140 (1983).
- [26] U. W. Heinz and P. F. Kolb, *Nucl. Phys. A* **702**, 269 (2002) [hep-ph/0111075].
- [27] M. L. Miller, K. Reygers, S. J. Sanders and P. Steinberg, *Ann. Rev. Nucl. Part. Sci.* **57**, 205 (2007) [nucl-ex/0701025].
- [28] E. Retinskaya, M. Luzum and J. Y. Ollitrault, *Phys. Rev. C* **89**, no. 1, 014902 (2014) [arXiv:1311.5339 [nucl-th]].
- [29] D. Teaney and L. Yan, *Phys. Rev. C* **83**, 064904 (2011) [arXiv:1010.1876 [nucl-th]].
- [30] R. S. Bhalerao, M. Luzum and J. Y. Ollitrault, *Phys. Rev. C* **84**, 034910 (2011) [arXiv:1104.4740 [nucl-th]].
- [31] H. Niemi, G. S. Denicol, H. Holopainen and P. Huovinen, *Phys. Rev. C* **87**, no. 5, 054901 (2013) [arXiv:1212.1008 [nucl-th]].
- [32] F. G. Gardim, J. Noronha-Hostler, M. Luzum and F. Grassi, arXiv:1411.2574 [nucl-th].
- [33] D. Teaney and L. Yan, *Phys. Rev. C* **86**, 044908 (2012) [arXiv:1206.1905 [nucl-th]].
- [34] F. G. Gardim, F. Grassi, M. Luzum and J. Y. Ollitrault, *Phys. Rev. C* **85**, 024908 (2012) [arXiv:1111.6538 [nucl-th]].
- [35] J. P. Blaizot, F. Gelis, J. F. Liao, L. McLerran and R. Venugopalan, *Nucl. Phys. A* **873**, 68 (2012) [arXiv:1107.5296 [hep-ph]].
- [36] T. Epelbaum, F. Gelis, N. Tanji and B. Wu, *Phys. Rev. D* **90**, no. 12, 125032 (2014) [arXiv:1409.0701 [hep-ph]].
- [37] G. Ferini, M. Colonna, M. Di Toro and V. Greco, *Phys. Lett. B* **670**, 325 (2009) [arXiv:0805.4814 [nucl-th]].
- [38] V. Greco, M. Colonna, M. Di Toro and G. Ferini, *Prog. Part. Nucl. Phys.* **62**, 562 (2009) [arXiv:0811.3170 [hep-ph]].
- [39] S. Plumari and V. Greco, *AIP Conf. Proc.* **1422**, 56 (2012) [arXiv:1110.2383 [hep-ph]].
- [40] S. Plumari, A. Puglisi, M. Colonna, F. Scardina and V. Greco, *J. Phys. Conf. Ser.* **420**, 012029 (2013) [arXiv:1209.0601 [hep-ph]].
- [41] M. Ruggieri, F. Scardina, S. Plumari and V. Greco, *Phys. Lett. B* **727**, 177 (2013) [arXiv:1303.3178 [nucl-th]].
- [42] Z. Xu and C. Greiner, *Phys. Rev. C* **71**, 064901 (2005) [hep-ph/0406278].
- [43] B. Zhang, M. Gyulassy and C. M. Ko, *Phys. Lett. B* **455**, 45 (1999) [nucl-th/9902016].
- [44] D. Molnar and M. Gyulassy, *Nucl. Phys. A* **697**, 495 (2002) [Erratum-ibid. *A* **703**, 893 (2002)] [nucl-th/0104073].
- [45] F. Retiere and M. A. Lisa, *Phys. Rev. C* **70**, 044907 (2004) [nucl-th/0312024].
- [46] L. Yan, J. Y. Ollitrault and A. M. Poskanzer, *Phys. Lett. B* **742**, 290 (2015) [arXiv:1408.0921 [nucl-th]].
- [47] A. K. Chaudhuri and U. W. Heinz, *J. Phys. Conf. Ser.* **50**, 251 (2006) [nucl-th/0504022].
- [48] W. Florkowski and R. Ryblewski, *Phys. Rev. C* **83**, 034907 (2011) [arXiv:1007.0130 [nucl-th]].
- [49] R. S. Bhalerao, A. Jaiswal, S. Pal and V. Sreekanth, *Phys. Rev. C* **89**, no. 5, 054903 (2014) [arXiv:1312.1864 [nucl-th]].
- [50] Y. Hatta, J. Noronha, G. Torrieri and B. W. Xiao, *Phys. Rev. D* **90**, no. 7, 074026 (2014) [arXiv:1407.5952 [hep-ph]].
- [51] S. S. Gubser and A. Yarom, *Nucl. Phys. B* **846**, 469 (2011) [arXiv:1012.1314 [hep-th]].
- [52] P. Staig and E. Shuryak, *Phys. Rev. C* **84**, 034908 (2011) [arXiv:1008.3139 [nucl-th]].
- [53] R. A. Lacey, A. Taranenko, J. Jia, D. Reynolds, N. N. Ajitanand, J. M. Alexander, Y. Gu and A. Mwai, *Phys. Rev. Lett.* **112**, no. 8, 082302 (2014) [arXiv:1305.3341 [nucl-ex]].

- [54] M. Gyulassy, I. Vitev, X. N. Wang and B. W. Zhang, In *Hwa, R.C. (ed.) et al.: Quark gluon plasma* 123-191 [nucl-th/0302077].
- [55] G. S. Denicol, J. Noronha, H. Niemi and D. H. Rischke, Phys. Rev. D **83**, 074019 (2011) [arXiv:1102.4780 [hep-th]].
- [56] M. P. Heller, R. A. Janik, M. Spalinski and P. Witaszczyk, Phys. Rev. Lett. **113**, no. 26, 261601 (2014) [arXiv:1409.5087 [hep-th]].